Interaction of ultrashort laser pulses and silicon solar cells under short circuit conditions

M. Mundus,[a] J. A. Giesecke, P. Fischer, J. Hohl-Ebinger, and W. Warta
Fraunhofer Institute for Solar Energy Systems (ISE), Heidenhofstraße 2, 79110 Freiburg, Germany

(Received 23 December 2014; accepted 11 February 2015; published online 24 February 2015)

Ultrashort pulse lasers are promising tools for numerous measurement purposes. Among other benefits their high peak powers allow for efficient generation of wavelengths in broad spectral ranges and at spectral powers that are orders of magnitude higher than in conventional light sources. Very recently this has been exploited for the establishment of sophisticated measurement facilities for electrical characterization of photovoltaic (PV) devices. As the high peak powers of ultrashort pulses promote nonlinear optical effects they might also give rise to nonlinear interactions with the devices under test that possibly manipulate the measurement outcome. In this paper, we present a comprehensive theoretical and experimental study of the nonlinearities affecting short circuit current (I_{SC}) measurements of silicon (Si) solar cells. We derive a set of coupled differential equations describing the radiation-device interaction and discuss the nonlinearities incorporated in those. By a semi-analytical approach introducing a quasi-steady-state approximation and integrating a Green's function we solve the system of equations and obtain simulated I_{SC} values. We validate the theoretical model by I_{SC} ratios obtained from a double ring resonator setup capable for reproducible generation of various ultrashort pulse trains. Finally, we apply the model to conduct the most prominent comparison of I_{SC} generated by ultrashort pulses versus continuous illumination. We conclude by the important finding that the nonlinearities induced by ultrashort pulses are negligible for the most common I_{SC} measurements. However, we also find that more specialized measurements (e.g., of concentrating PV or Si-multijunction devices as well as highly localized electrical characterizations) will be biased by two-photon-absorption distorting the I_{SC} measurement. © *2015 AIP Publishing LLC*. [http://dx.doi.org/10.1063/1.4913394]

I. INTRODUCTION

Driven by the further development of solar cell technologies and the scientifically as well as economically motivated demand for lower measurement uncertainties the characterization and calibration of solar cells is a field of steady research. The commercialization of ultrashort pulse lasers within the last decades opened new opportunities to meet this demand by innovative and highly sophisticated measurement facilities. Exploiting the high peak powers of ultrashort pulse lasers a coherent supercontinuum can be generated that has very recently been used as light source for novel solar simulators and device characterization facilities.[1] In other approaches, the ultrashort pulses are applied to generate spectrally tunable, quasi-monochromatic radiation by nonlinear optical effects. The unprecedented average spectral power is used for highly sophisticated external quantum efficiency and solar cell calibration facilities with improved accuracy and resolution at extended spectral ranges.[2–4]

The assurance that ultrashort pulses and continuous illumination yield identical measurement results is vital for the application of such radiation sources in ambitious measurement facilities. As the ultrashort pulse lasers that are typically used for such applications exhibit pulse repetition rates in the 100 MHz-regime they are often referred to as quasi-continuous radiation sources. Indeed it has been shown that changes in the repetition rate have negligible impact on measurements.[1] However, not only the pulse repetition rate but also the tight temporal confinement of photons within a pulse duration might affect the measurement outcome.[5] As this confinement promotes nonlinear optical effects required for wavelength conversions it might also give rise to nonlinearities within the tested devices. For instance, two-photon absorption (TPA) and saturation in carrier generation may contribute to the overall excess charge carrier density. Moreover, pulsed excitation is intrinsically tied to variations of carrier densities within a pulse period. Hence, carrier density dependent lifetime effects might affect the measurement.

In order to avoid these potential nonlinearity problems various procedures for temporal shaping of laser pulses have been developed in the past.[6–8] However, to the best of our knowledge, the impact of ultrashort laser pulses on measurements of photovoltaic devices has not been investigated yet. Thus, the necessity of these ambitious temporal pulse shapers for the electrical characterization of photovoltaic devices is yet neither proven nor disproven.

In this paper, we will close this gap by a theoretical and experimental investigation of potential nonlinearities in short circuit current (I_{SC}) measurements of a silicon (Si) solar cell. Firstly, we derive a theoretical framework for I_{SC} computation based on coupled differential equations describing the evolution of excess charge carriers and ultrashort pulse radiation intensity. From this set of equations, we identify those nonlinearities that might affect the excess carrier density

[a]Author to whom correspondence should be addressed. Electronic mail: markus.mundus@ise.fraunhofer.de

and, hence, the I_{SC}. For retrieving the I_{SC} from the differential equations we introduce a quasi-steady-state approximation and use a Green's function approach. Afterwards, we confirm these simulations by experimental results obtained from a double ring resonator setup for redistribution of pulse energy within a pulse period. Finally, we apply the theoretical model to answer the most urgent but experimentally hardly accessible question of I_{SC} deviations under ultrashort laser pulse excitation as compared to continuous illumination.

II. THEORETICAL

A. Modeling short circuit current under ultrashort laser pulses

For the derivation of a model capable of predicting I_{SC} values for different illumination and sample characteristics we start by describing the I_{SC} in terms of excess charge carrier density Δn. As the I_{SC} is defined by the current flow at zero voltage across the device junction, it is proportional to the gradient of Δn at the junction ($z=0$) for an effective front surface recombination velocity $S_0 \rightarrow \infty$ (SRV). Thus,

$$I_{SC} \propto \left.\frac{d\Delta n}{dz}\right|_{\substack{z=0 \\ S_0\rightarrow\infty}} \tag{1}$$

for front junction solar cells. In the first instance, Δn is proportional to the generation rate of excess charge carriers G. However, although less prominent than under open circuit conditions excess carrier recombination competes with the extraction of charge carriers. Thus, for a rigorous computation of Δn, the continuity equation

$$\frac{\partial \Delta n(z,t)}{\partial t} = D_a \frac{\partial^2 \Delta n}{\partial z^2} + G - \frac{\Delta n}{\tau(\Delta n)} \tag{2}$$

with ambipolar diffusion coefficient D_a and excess carrier lifetime $\tau(\Delta n)$ needs to be applied. The excess carrier generation rate G, taking into account TPA, reads

$$G = \left(\sigma_\alpha (N_0 - \Delta n) + \sigma_\beta (N_0 - \Delta n)\frac{I}{2}\right)\frac{I}{h\upsilon}. \tag{3}$$

Here, σ_α (in cm^2) and σ_β (in cm^4/W) denote the linear and nonlinear band-to-band absorption cross-sections, N_0 the density of states, I the radiation intensity, h Planck's constant, and ν the radiation frequency. It has to be noted that for computation of absolute Δn and, thus, I_{SC} values consideration of light trapping effects might be required in Eq. (3).[9] However, as the discussion in Sec. IV is restricted to I_{SC} ratios it can be shown that light trapping is mostly negligible as the generation term is either dominated by linear or nonlinear band-to-band carrier generation.

From Eqs. (2) and (3), three potential nonlinearities contributing to deviating excess carrier densities for pulsed versus continuous illumination can be identified. Firstly, the term $(N_0 - \Delta n)$ in Eq. (3) acts as a saturation of carrier generation for Δn approaching N_0. As for short circuit conditions Δn typically ranges from 10^{12} cm^{-3} to 10^{14} cm^{-3} (at 1 sun), $(N_0 - \Delta n) \approx N_0$ is generally assumed. However, for ultrashort pulse excitation, the virtually instantaneous generation of excess carriers must be considered as it possibly violates the approximation $\Delta n/N_0 \ll 1$. For the experimental conditions of this work even the most conservative treatment of a non-depth averaged generation rate yields an additional excess carrier dose by a single pulse well below 10^{17} cm^{-3}, so that $\Delta n/N_0 \ll 1$ remains valid. Consequently, Eq. (3) can be simplified to

$$G = \left(\alpha + \beta\frac{I}{2}\right)\frac{I}{h\upsilon}, \tag{4}$$

with linear absorption coefficient $\alpha = \sigma_\alpha N_0$ and TPA coefficient $\beta = \sigma_\beta N_0$.

Secondly, the temporally confined carrier generation by an ultrashort pulse leads to intrinsic variations in Δn within a pulse period. With τ being dependent on Δn (see Eq. (2)) a different effective minority carrier lifetime τ_{eff} and, hence, recombination rate $\Delta n/\tau_{eff}$ might arise for pulsed as compared to continuous illumination. However, it can be shown that the additional change of excess carrier density due to injection-dependent carrier lifetime is negligible compared to the overall change of excess carrier density within an ultrashort pulse period T, as $\tau \gg T$. Such reasoning is valid even in the most extreme case of open circuit conditions. Then, any reduction of excess carrier density is induced by excess carrier recombination, whereas under short circuit conditions carrier extraction is much more dominant than carrier recombination. Therefore, Eq. (2) can be written as

$$\frac{\partial \Delta n(z,t)}{\partial t} = D_a \frac{\partial^2 \Delta n}{\partial z^2} + \left(\alpha + \beta\frac{I}{2}\right)\frac{I}{h\upsilon} - \frac{\Delta n}{\tau}. \tag{5}$$

Finally, TPA appears as a nonlinear term in Eqs. (3) and (4). As TPA does not depend on Δn its contribution to the overall carrier density cannot be readily neglected by straightforward considerations as above and, thus, remains as the only nonlinear contribution in Eqs. (3) and (4).

B. Quasi-steady-state approximation

The radiation intensity I used in Eqs. (3) and (5) can be written as[10]

$$\frac{\partial I(z,t)}{\partial z} = -\big(\alpha + \beta I(z,t) + \sigma_{FCA}(n+p)\big)I(z,t). \tag{6}$$

In addition to the previously introduced linear and nonlinear absorption coefficients α and β, the free carrier absorption (FCA) cross section σ_{FCA} appears in Eq. (6). It describes pulse intensity reduction due to an energy transfer from the incident photons to any free carriers.[11,12] FCA is of particular importance as it causes coupling of Eqs. (5) and (6) by the carrier densities $n = n_0 + \Delta n$ and $p = p_0 + \Delta n$ (with n_0 and p_0 as doping densities of n- or p-type Si, respectively).

As this coupling involves tremendous computational effort for solving the set of differential equations we introduce a quasi-steady-state approximation that yields a decoupling of the differential equations (5) and (6). This

approximation relies on the following two assumptions: firstly, changes in FCA by a *single* ultrashort pulse have a negligible effect on the absorption conditions for the pulse *itself*; secondly, carrier redistribution by diffusion is sufficiently slow to be neglected for the time scale at which an ultrashort pulse travels through the sample.

Regarding the first assumption, we argue that if a *single* ultrashort pulse induces significant changes in FCA (equivalent to a significant increase in Δn by this single pulse), the FCA is dominated by linear band-to-band absorption and, hence, can be neglected in Eq. (6). On the contrary if the induced changes in FCA are faint (small increase in Δn) the changes itself are negligible. Therefore, the changes in FCA induced by a single ultrashort pulse do not affect the pulse itself. Consequently, the excess carrier distribution created by the ensemble of all preceding pulses can be used just as well for solving Eq. (6). It is noteworthy that this assumption might be violated at illumination intensities exceeding 1 kW/cm^2 and wavelengths in the vicinity of the Si band edge as the change in FCA by a single pulse might be significant compared to the linear band-to-band absorption.

For the second assumption, we estimate the carrier redistribution by diffusion within a pulse transit time through a sample to be smaller than 0.1 μm. As this distance is much smaller than the spatial discretization of some μm that is typically applied in numerical simulations, we argue that carrier redistribution can be neglected for the time a pulse travels through the sample.

With both assumptions combined we achieve a steady-state excess carrier distribution $\Delta n(z)$ that is known prior to the interaction of each ultrashort pulse with the target solar cell. Thus, Eq. (6) can be solved by

$$I(z,t) = \frac{I(t)\alpha_{\mathrm{tot}}(z)\exp(-\alpha_{\mathrm{tot}}(z)z)}{\alpha_{\mathrm{tot}}(z) + \beta I(t)(1-\exp(-\alpha_{\mathrm{tot}}(z)z))}, \qquad (7)$$

with $\alpha_{\mathrm{tot}}(z) = \alpha + \sigma_{\mathrm{FCA}}(n(z)+p(z))$ and directly inserted into Eq. (5).

Within the constraints given above Eqs. (5) and (7) can be used to simulate ultrashort pulse interaction with solar cells (note that this is not necessarily limited to short circuit conditions). However, as shown in Eq. (1) a comparably high front SRV is required for modeling short circuit conditions. As such strongly confined recombination (or in this case extraction) properties require narrow discretization for finite element simulations in both space and time, we applied a Green's function approach to obtain a semi-analytical solution to the set of equations. The approach is sketched in the Appendix and motivated in Ref. 13.

C. Deviation in linear and nonlinear excess carrier generation rate

Prior to experimental verifications of the theoretical framework discussed above it is beneficial to identify spectral regions and illumination intensities that potentially yield a significant impact of TPA on I_{SC} measurements. Therefore, an analytical estimation of its impact based on the generation term given in Eq. (4) is conducted. For this the nonlinear generation rate $G_{\mathrm{NL}} = \beta I^2/(2h\nu)$ is compared to the linear generation rate $G_{\mathrm{L}} = \alpha I/(h\nu)$ by

$$\frac{G_{\mathrm{NL}}}{G_{\mathrm{L}}} = \frac{\beta}{2\alpha} I_{0,\mathrm{rect}} = \frac{\beta}{2\alpha} \frac{I_{\mathrm{av}}}{f_{\mathrm{rep}}\tau_{1/e^2}}. \qquad (8)$$

Here, $I_{0,\mathrm{rect}} = P_{0,\mathrm{rect}}/A$ (with illuminated area A) denotes the peak intensity of an ultrashort laser pulse converted from its Gaussian pulse shape to a rectangular shape of equivalent pulse energy $E_{\mathrm{pulse}} = P_{\mathrm{av}}/f_{\mathrm{rep}}$ and pulse duration τ_{1/e^2}. P_{av} is the average laser power of a train of such pulses at a repetition rate of f_{rep}.

With material data from Green and Keevers[14] and Bristow *et al.*[15] for linear and nonlinear absorption coefficients in intrinsic silicon the deviation in excess carrier generation is computed for common ultrashort pulse laser parameters of $f_{\mathrm{rep}} = 80$ MHz and $\tau_{1/e^2} \approx 170$ fs (Fig. 1). As the linear absorption coefficient reduces for longer wavelengths an increase of the TPA impact is observed, especially for those wavelengths in the vicinity of the material band edge. For shorter wavelengths, TPA is clearly dominated by linear absorption processes.

Consequently, for an experimental evidence for contribution of TPA to the I_{SC} wavelengths in the spectral range above 1150 nm should be considered.

III. EXPERIMENTAL

A. Experimental setup

For generation of ultrashort laser pulses at wavelengths longer than 1150 nm we apply an optical parametric oscillator (OPO) (Inspire/Newport Spectra-Physics) pumped by the frequency-doubled radiation of a titanium-sapphire ultrashort pulse laser (MaiTai/Newport Spectra-Physics). The OPO emits pulses of approximately 150 fs pulse duration at 80 MHz repetition rate, spectrally tunable from 900 nm to 2500 nm.

For a reliable experimental demonstration of TPA impact on I_{SC} measurements, we regard the variation of pulse energy distribution within a pulse period at slightest changes of the geometrical radiation properties as the most

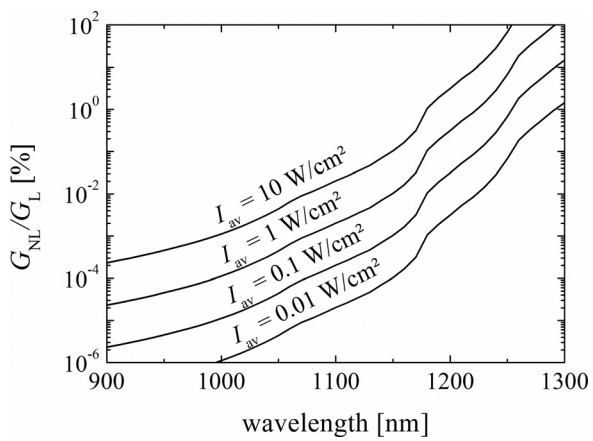

FIG. 1. Deviation of nonlinear excess carrier generation rate G_{NL} to linear excess carrier generation rate G_{L} for various average illumination intensities I_{av}. The impact of G_{NL} rises with increasing wavelength and intensity.

crucial requirement. Therefore, we equipped a standard I_{SC} measurement configuration consisting of a chopper wheel, a lock-in amplifier and a transimpedance amplifier with two ring resonators for redistribution of pulse energy (Fig. 2).

An incoming pulse is partially transmitted by the beam splitter of the first ring resonator (after passing through a chopper wheel and a beam sampler for monitoring purposes) and temporally delayed with respect to its reflected complement. The temporal delay can be adjusted by a translation stage that varies the cavity length of the ring resonator to μm-precision. After one roundtrip in the ring cavity, the pulse hits the beam splitter again and is another time partially transmitted and partially reflected. If the roundtrip time of the ring cavity equals half of the pulse period a pulse does temporally coincide with the subsequently emitted pulse of the OPO after two cavity roundtrips. Consequently, the pulse after one cavity roundtrip is located exactly in between the two consecutive OPO pulses. This is a very favorable situation regarding the conceptual simplicity of the setup. It allows for the creation of a second pulse that carries as much energy as the partially reflected original pulse and that is temporally located exactly in between two consecutive pulses of the OPO. For this to be achieved, a second, identical ring resonator needs to be implemented and appropriate beam splitter ratios need to be chosen. Once precisely adjusted the double ring resonator configuration can be regarded as an optical element that doubles the pulse repetition rate of the laser source by redistributing one half of an incoming pulse's energy to the temporal center between two consecutive pulses.

In order to achieve the necessary precise alignment in space and time, both, temporal and spatial alignments are monitored by an autocorrelator and a camera. Additionally, a monitor diode tracks laser intensity fluctuations.

We chose this setup as it enables effortless redistribution of pulse energy without severe changes to the geometrical radiation properties by slight misalignments of the translation stages. For instance, a cavity length misalignment of 100 μm induces a change in temporal delay by 334 fs, so that pulses of 150 fs pulse duration do not temporally overlap anymore. At the same time, the impact of this slight change of cavity length on the radiation geometry (e.g., beam diameter at focusing lens, pointing direction) is faint.

For validation of the spatio-temporal overlap of the pulses camera images and autocorrelation traces are shown in Fig. 3. The good spatial alignment is obvious from the camera images that display a single spot. Slight spatial misalignments would result in multiple spots on camera and target (not shown here). In the image representing the temporally aligned case (right image) interference fringes can be observed. Because of air and setup vibrations the spatial positions of these fringes are subject to continuous variations that we observed during the experiment. A slight misalignment of the translation stages eliminates the appearance of the fringes (left image).

Knowing that the coherence function of an ultrashort pulse train does only allow for interference in case of a temporal overlap of the pulses the camera image is a strong proof for the good temporal alignment of the setup as well. However, for clarity autocorrelation measurements for varying cavity lengths are also shown in Fig. 3. For misaligned cavities (left) multiple peaks in the autocorrelation trace can be observed that merge when the cavities are aligned (left to right). The temporal overlap of the individual pulses emitted by the double ring resonator configuration is also evident from the increased background noise in the aligned case that origins from interference in the collinearly configured autocorrelator.

In order to achieve the high illumination intensities required for the experimental proof of TPA we focus the radiation by a lens with 200 mm focal length to a spot of

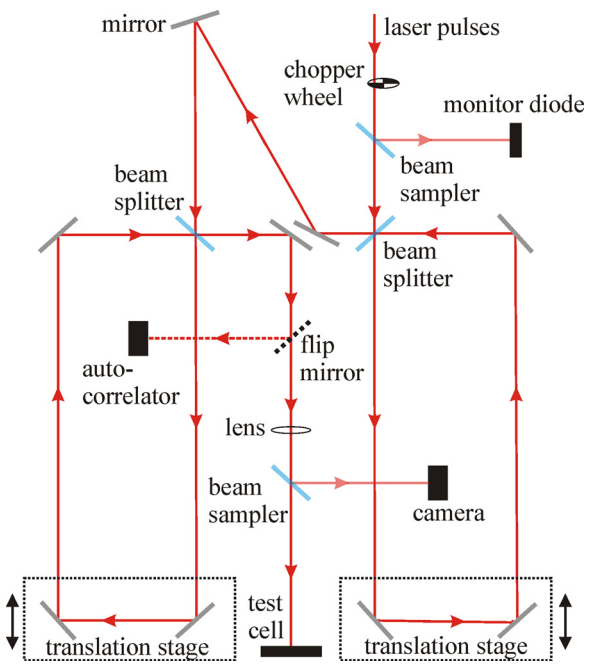

FIG. 2. Schematic drawing of the optical setup of the double ring resonator experiment. An incident pulse is divided into several temporally separated but spatially aligned pulses. The relative temporal delay of the pulses can be controlled by translation stages.

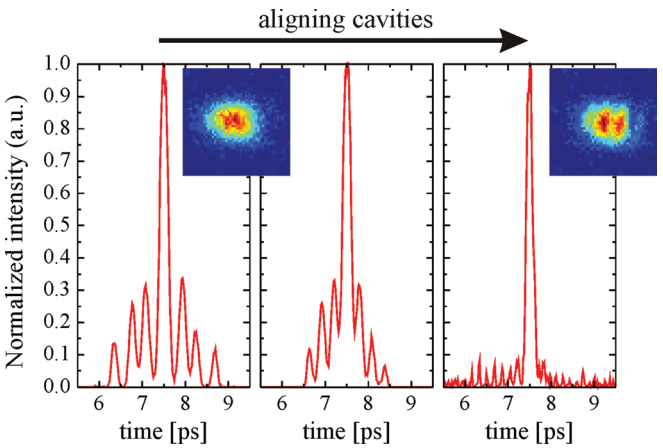

FIG. 3. Autocorrelation (AC) measurements and camera images of the laser spot for validation of spatio-temporal overlap of ultrashort laser pulses after the double ring resonator setup. When aligning the cavity lengths the AC traces merge to a single pulse (from left to right) and interference fringes in the camera image of the laser spot (top right) are observed.

approximately 150 μm diameter. With average optical powers of about 20 mW we obtain illumination intensities of approximately 100 W/cm^2.

As solar cell sample we used a 200 μm thick 2 × 2 cm^2 n-type silicon solar cell with $n_0 = 5{\cdot}10^{15}$ cm^{-3}.

B. Experimental results

As a preliminary test for functionality of our setup we set a wavelength of 1300 nm and measured the I_{SC} of the target solar cell for different ring resonator cavity lengths (Fig. 4). By this variation different pulse energy distributions have been obtained that are illustrated by the inset shown in Fig. 4. If both cavity lengths are aligned to match twice the pulse repetition frequency two pulses of equal amplitudes separated by half of the pulse period are obtained (shown in green at top). Misaligning both cavities identically yields a partial coincidence of some pulses (blue/middle), whereas a different misalignment of the two cavities yields the maximum achievable pulse energy redistribution (red/bottom). From the changes in I_{SC} with variation of pulse energy distributions a clear nonlinearity is readily deduced as the overall optical power is constant over the measurements and minor intensity fluctuations are corrected. The two misaligned cases differ in their I_{SC} as in the identically misaligned case less pulses at higher pulse peak powers are present owing to the partial temporal coincidence of some of the pulses. Moreover, the step-like result demonstrates robustness and reproducibility of our experimental approach as previous I_{SC} values can be restored by simple readjustment of cavity lengths. The increased noise for a perfect temporal overlap of the pulses is another evidence for the precise temporal match of the partial pulses as it is caused by interference of the radiation on the solar cell target.

Carrying out this analysis for various wavelengths from 1200 nm to 1650 nm we obtain the results shown in Fig. 5. The green triangles denote the measured I_{SC} for aligned cavity lengths, the red squares for misaligned cavity lengths. For all wavelengths, the misaligned measurement delivers significantly less I_{SC} than the aligned measurement which demonstrates a significant impact of nonlinear absorption. Moreover, the relative change in I_{SC} over wavelength is

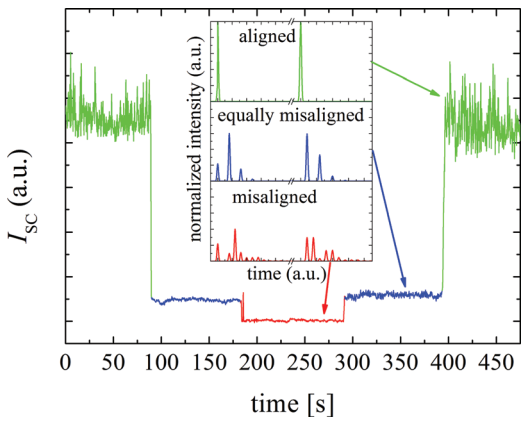

FIG. 4. I_{SC} measurement for different lengths of the ring resonator cavities. By changes of the cavity lengths different pulse energy distributions are achieved (schematically shown in inset) resulting in diverse I_{SC} values.

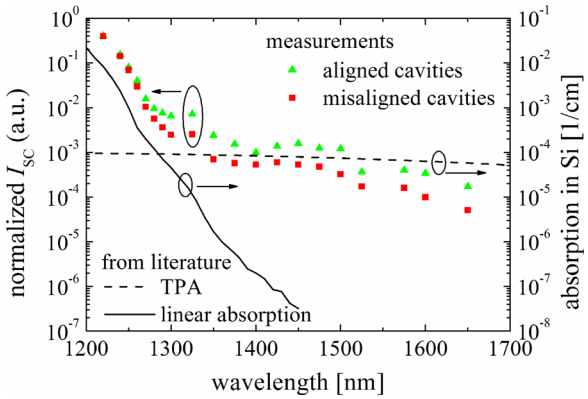

FIG. 5. Comparison of I_{SC} measurements for aligned (green triangles) and misaligned cavity lengths (red squares) over wavelength plus linear (solid line) and nonlinear (TPA) absorption (dashed line) from literature.[14,15]

reduced when the radiation wavelength is increased. This imitates the change from dominating linear absorption that is monotonically decreasing with wavelength (solid line; values from Ref. 14) to dominating nonlinear absorption (dashed line; values from Ref. 15 with pulse properties as applied in the experiment). We take this as experimental evidence for TPA as the origin of the nonlinearity observed in the I_{SC} measurements.

IV. SIMULATIONS

For validation of our numerical approach presented above, we modeled the ultrashort pulse trains as created by the experimental setup described in Sec. III A and applied them as $I(t)$ to Eqs. (4) and (7). By solving for the excess carrier density distribution $\Delta n(z,t)$ using the Green's function approach discussed in the Appendix we retrieved the I_{SC} for the aligned and the misaligned case from Eq. (1). By taking the ratio of both, we eliminated the proportionality factor. We accounted for the limited alignment precision of the ring resonator cavities by a normal distribution with an estimated standard deviation of 10 μm around the perfect alignment position. At each wavelength 1000 I_{SC} ratios have been simulated with randomized translation stage misalignments according to the described normal distribution.

Simulated and experimental results are shown in Fig. 6. The black open and filled squares are experimental I_{SC} ratios, the red curve represents the average I_{SC} ratios after 1000 simulations with randomized stage deviations. Standard deviations are included as error bars (attached to the black squares) and the reddish area around the mean simulated I_{SC} ratio.

The simulations show a good agreement to the experimental data. Especially the data ranging from 1200 nm to 1350 nm demonstrate excellent conformity. Even for longer wavelengths and, thus, lower measurement signals a quite good agreement to most of the data points is obtained. However, some measurement values are not captured by the simulations. We attribute this to remaining deviations of the experimental conditions to the simulation input data as not all experimental parameters could have been precisely determined (e.g., pulse duration and input power). From the

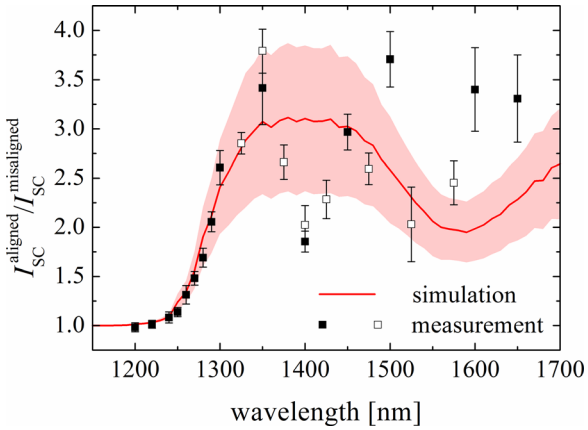

FIG. 6. Comparison of experimental to simulated ratios of I_{SC} in aligned and in misaligned cavity configuration. Numerical simulations and measurement data show a good agreement.

matter of fact that the most apparent property of the measurements, the slope from 1250 nm to 1350 nm, is imitated to a very good degree we conclude that our simulations are able to reproduce and describe the experiments.

Consequently, we deduce that our numerical model is eligible for predictions on the most urgent but experimentally hardly accessible comparison of continuous to ultrashort pulsed illumination. For this comparison, we modeled typical ultrashort pulses of 100 fs pulse duration and 80 MHz pulse repetition rate at varying illumination intensities and compared the resulting I_{SC} to the one obtained from continuous illumination at equivalent optical powers (Fig. 7). The significance of nonlinear absorption is drastically increased for longer wavelengths, especially at high concentrations. However, within the spectral ranges and illumination intensities Si solar cells are commonly characterized ($\lambda \leq 1200$ nm, intensity < 0.1 W/cm^2) the deviations are below 0.1% and can be neglected, especially when taking into account the contribution of this spectral region to the integrated I_{SC} of the cell.

From this point of view, common electrical characterizations of today's single-junction Si solar cells can be accomplished without usage of highly sophisticated tools for

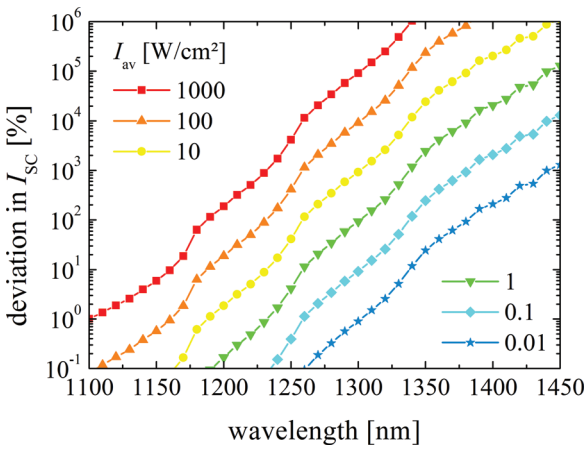

FIG. 7. Deviation of the I_{SC} of a Si solar cell illuminated with 100 fs ultrashort pulses at 80 MHz repetition rate as compared to continuous illumination at identical average intensity.

temporal shaping of the ultrashort laser pulses. However, when the radiation is highly concentrated and, hence, higher illumination intensities are obtained (e.g., in local electrical characterizations or in concentrating photovoltaics) the TPA contribution to the I_{SC} needs to be taken into account.

V. CONCLUSIONS

In conclusion, we have presented a comprehensive study of potential nonlinearities in Si solar cells at short circuit conditions when irradiated with ultrashort pulses. By an experimental approach that enabled convenient pulse energy redistribution we succeeded in experimental demonstration of TPA impact on the I_{SC} of the solar cell. We applied the experimental results to validate a theoretical model based on both a Green's function approach and a quasi-steady-state approximation to solve a set of differential equations describing the radiation-semiconductor interaction.

With this experimentally validated model, we were able to simulate the comparison of ultrashort pulse excitation to continuous wave excitation of Si solar cells, which is experimentally hardly accessible. We have drawn the important conclusion that I_{SC} measurements of Si solar cells with illumination intensities lower than 0.1 W/cm^2 are not significantly affected by nonlinearities. Thus, ultrashort laser pulses can be readily used for such applications. However, at higher concentrations (for local electrical characterization or in concentrating PV), TPA can have significant impact on the measurement results.

The presented analysis and the drawn conclusions are restricted to Si solar cells. Alternative materials with other linear and nonlinear absorption characteristics might react differently to ultrashort pulse excitation regarding TPA. Moreover, for the emerging PV technologies, especially the advanced PV concepts including Si-multijunction and down- and up-converters,[16,17] the ultrashort laser pulses can yield a misinterpretation of the device characteristics by TPA induced current contributions generated in the Si-part of the devices.

Therefore, we like to conclude by recommending temporal shaping of ultrashort laser pulses in measurement facilities for electrical characterization of solar cells. These temporal shapers should convert the pulses into continuous radiation or at least enlarge the pulse durations significantly. Although we have shown that the electrical characterization of standard Si solar cells is not harmed by the properties of the ultrashort pulses our results have as well demonstrated that nonlinearities do occur. Thus, without temporal shaping of ultrashort laser pulses other than standard applications of the new measurement facilities require a detailed analysis of potential nonlinear effects prior to the measurement.

ACKNOWLEDGMENTS

We gratefully acknowledge fruitful collaboration with Elisabeth Schäffer, Stephen Thomas Haag, Tim Niewelt and Bernhard Michl. This work was partially supported by the German Federal Ministry for the Environment, Nature Conservation and Nuclear Safety (Contract No. 0325242, TF-CalLab).

APPENDIX: GREEN'S FUNCTION APPROACH

Accurately modelling of short circuit conditions requires incorporation of a comparably high front SRV (see Eq. (1)). As stated above, such high SRVs readily yield tremendous computational effort as the strongly confined surface recombination properties require narrow spatial discretization Δz, that in turn requires narrow temporal discretization Δt, which greatly enhances computational effort in fully numerical approaches.[13]

In order to overcome this bottleneck, we applied a semi-analytical approach by using a Green's function of the heat equation. With this the impact of carrier diffusion can be treated analytically so that a much larger spatial discretization is applicable. Furthermore, the Green's function approach is especially advantageous for ultrashort pulses as the only relevant times for the simulation of Δn are those at which carrier generation takes place. As ultrashort pulse durations range between some hundred femtoseconds to several picoseconds, whereas the pulse periods are in the nanosecond regime, the relevant modeling times for the solution of Δn are very short compared to the overall pulse period. For instance, in our experimental conditions, the duty cycle of the ultrashort pulse train is below $7{\cdot}10^{-4}$. This led us to the conclusion that integration of the Green's function approach is most appropriate for solving Eq. (5) (with Eq. (7)) at a reasonable simulation effort.

After this short motivation for usage of the Green's function we briefly sketch the approach along the lines of Ref. 13 in the following. For more detailed information, the reader is referred to Refs. 13, 18, and 19.

In our approach, the excess carrier density distribution takes the form

$$\Delta n(z,t) = \int_0^t dt' \int_0^d d\zeta G(\zeta,t')\Gamma(z,\zeta,t-t')\exp\left(\frac{t'-t}{\tau}\right), \quad \text{(A1)}$$

with auxiliary variables ζ and t' describing space and time, respectively, and the Green's function

$$\Gamma(z,\zeta,t) = \sum_{n=1}^{\infty} \frac{y_n(z)y_n(\zeta)}{\|y_n\|^2}\exp\left(-\lambda_n^2 D_a t\right). \quad \text{(A2)}$$

The function y_n is given by

$$y_n(z) = \cos(\lambda_n z) + \frac{S_0}{D_a\lambda_n}\sin(\lambda_n z), \quad \text{(A3)}$$

with

$$\|y_n\|^2 = \frac{S_d}{2D_a\lambda_n^2}\frac{D_a^2\lambda_n^2+S_0^2}{D_a^2\lambda_n^2+S_d^2} + \frac{S_0}{2D_a\lambda_n^2} + \frac{d}{2}\left(1+\left(\frac{S_0}{D_a\lambda_n}\right)^2\right) \quad \text{(A4)}$$

as well as front SRV S_0, back SRV S_d, cell thickness d, diffusion coefficient D_a and the solution λ_n of the transcendental equation

$$\frac{\tan(\lambda_n d)}{\lambda_n} = \frac{D_a(S_0+S_d)}{D_a^2\lambda_n^2 - S_0 S_d}, \quad \text{(A5)}$$

defining the decay time of any mode n of excess carrier decay.

The carrier generation term $G(\zeta,t')$ is given by Eqs. (4) and (7) with $I(t)$ describing the specific temporal intensity distribution of the ultrashort pulse train.

[1] T. Dennis, J. B. Schlager, and K. A. Bertness, IEEE J. Photovolt. **4**, 1119 (2014).
[2] S. Winter, T. Fey, D. Friedrich, I. Kröger, and K. Von Volkmann, in *Proceedings of the 26th European Photovoltaic Solar Energy Conference and Exhibition, Hamburg, Germany, 2011*, p. 3466.
[3] S. Winter, T. Fey, I. Kröger, D. Friedrich, K. Ladner, B. Ortel, S. Pendsa, and F. Witt, Measurement **51**, 457 (2014).
[4] M. Mundus, D. Lill, J. Hohl-Ebinger, and W. Warta, in *Proceedings of the 29th European Photovoltaic Solar Energy Conference and Exhibition, Amsterdam, The Netherlands, 2014*, p. 3439.
[5] J. Mitchell, D. Hanna, R. Ullmann, A. Bamberger, A. Freidhof, M. Bräunig, G. Theisen, T. Trefzger, J. Lim, and B. Oh, Nucl. Phys. B-Proc. Suppl. **32**, 106 (1993).
[6] D. Hanna and J. W. Mitchell, Nucl. Instrum. Methods Phys. Res. Sec. A **324**, 14 (1993).
[7] R. Khare, P. Shukla, G. Mishra, C. Mukherjee, S. Talwar, V. Dubey, P. Saxena, and J. Mittal, Opt. Commun. **282**, 3850 (2009).
[8] R. Khare and P. K. Shukla, in *Coherence and Ultrashort Pulse Laser Emission*, edited by F. J. Duarte (InTech, 2010).
[9] P. A. Basore, in *Proceedings of the 23rd IEEE Photovoltaic Specialists Conference, Louisville, Kentucky, USA* (IEEE, New York, USA, 1993), p. 147.
[10] S. Fathpour, K. K. Tsia, and B. Jalali, IEEE J. Quantum Electron. **43**, 1211 (2007).
[11] D. Schroder, R. N. Thomas, and J. C. Swartz, IEEE J. Solid-State Circuits **13**, 180 (1978).
[12] M. Rüdiger, J. Greulich, A. Richter, and M. Hermle, IEEE Trans. Devices **60**, 2156 (2013).
[13] J. Giesecke, *Quantitative Recombination and Transport Properties in Silicon from Dynamic Luminescence* (Springer, 2014).
[14] M. A. Green and M. J. Keevers, Prog. Photovolt.: Res. Appl. **3**, 189 (1995).
[15] A. D. Bristow, N. Rotenberg, and H. M. Van Driel, Appl. Phys. Lett. **90**, 191104 (2007).
[16] K. Derendorf, S. Essig, E. Oliva, V. Klinger, T. Roesener, S. P. Philipps, J. Benick, M. Hermle, M. Schachtner, and G. Siefer, IEEE J. Photovolt. **3**, 1423 (2013).
[17] S. Fischer, J. Goldschmidt, P. Löper, G. Bauer, R. Brüggemann, K. Krämer, D. Biner, M. Hermle, and S. Glunz, J. Appl. Phys. **108**, 044912 (2010).
[18] A. D. Polyanin, *Handbook of Linear Partial Differential Equations for Engineers and Scientists* (CRC press, 2010).
[19] J. Giesecke and W. Warta, Appl. Phys. Lett. **104**, 082103 (2014).